Macromolecules

ARTICLE

pubs.acs.org/Macromolecules

Supramolecular Functionalization of Single-Walled Carbon Nanotubes (SWNTs) with Dithieno[3,2-*b*:2′,3′-*d*]pyrrole (DTP) Containing Conjugated Polymers

Patigul Imin, Mokhtar Imit, and Alex Adronov*

Department of Chemistry and Chemical Biology, the Brockhouse Institute for Materials Research, McMaster University, Hamilton, Ontario, Canada

Supporting Information

ABSTRACT: Fluorene and dithieno[3,2-*b*:2′,3′-*d*]pyrrole (DTP) containing conjugated polymers, {2,7-[9,9-didodecylfluorene]-*alt*-2,6-[*N*-dodecyldithieno(3,2-*b*:2′,3′-*d*)pyrrole]} (PF-DTP1) and {2,7-[9,9-didodecylfluorene]-*alt*-2,6-[*N*-3,4,5(*n*-dodecyloxy)phenyl-dithieno(3,2-*b*:2′,3′-*d*)pyrrole]} (PF-DTP2), have been successfully synthesized using Suzuki polycondensation. These polymers possess excellent thermal stability with decomposition temperatures over 365 °C under Ar. The introduction of soluble side chains on the DTP units and incorporation with soluble dialkyl-substituted fluorene resulted in highly soluble polymers with novel optoelectronic properties. The supramolecular complex formation of these DTP containing polymers with single-walled carbon nanotubes (SWNTs) has been studied, and it was found that these polymers can form strong supramolecular polymer−nanotube assemblies and produce stable complexes in solution. UV−vis−NIR absorption, photoluminescence excitation (PLE), and Raman spectroscopy were used for the characterization and identification of the nanotube species that are present in THF solution. The strong nanotube emission was observed from individual SWNTs even after removal of excess free polymer by filtration and washing. On the basis of these two polymers, it was found that the interactions with the SWNT surface are more strongly dictated by the polymer backbone than the side chain, though further studies may be warranted.

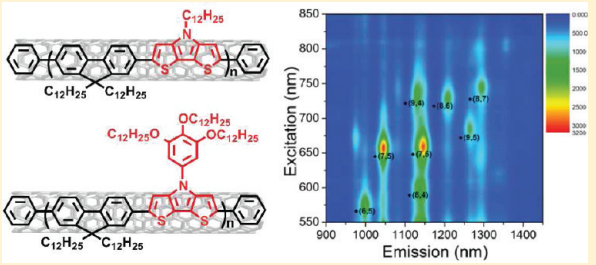

INTRODUCTION

Single-walled carbon nanotubes (SWNTs) are of special interest in current research due to their extraordinary mechanical, electronic, and optical properties.[1−5] Their unique structure, remarkable thermal and electrical conductivity, and high mechanical strength make SWNTs viable candidates for a wide range of device applications, including chemical sensors,[6−8] field-effect transistors,[9] nanoscale integrated radio receivers,[10,11] photovoltaics,[12−14] and field-emission displays.[3,15] However, the inherent insolubility of carbon nanotubes in most organic and aqueous solvents has hindered the widespread application of these novel nanostructures. Therefore, a great deal of research has been focused on functionalization of SWNTs, mainly to enhance their solubility and solution phase processability.[5,16,17] The supramolecular functionalization methodology has received much recent attention because this approach does not introduce any defects in the nanotube side wall, thus preserving the electrical and mechanical properties of the resulting materials.[18−20]

Recently, it has been shown that various conjugated polymers form strong supramolecular complexes with SWNTs, enabling their dissolution in organic solvents, as well as water, depending on the nature of the side chain.[19,21−28] Among all conjugated polymers, fluorene- and thiophene-containing conjugated polymers are of particular interest due to their good solubility, processability, and unique optoelectronic properties.[14,26,29−36] Recently, it has been found that fluorene- and thiophene-containing conjugated polymers can form stable complexes with SWNTs and exhibit excellent solubility and solution stability properties even after removal of excess free polymer.[27,29] Interest in this class of conjugated polymers has gained much recent popularity as reports of selective solubilization of certain SWNT species have begun to be published.[20,30,31,37,38] It is therefore desirable to develop a detailed understanding of how variations in the backbone or the side chain of a conjugated polymer can affect the interactions between the polymer and the SWNT surface. In particular, structural components that increase the strength of polymer binding to the nanotube surface are of significant interest. Although the fused-ring precursors of poly(thiophene)s should result in stronger nanotube binding behavior when compared to the previously reported alkylthiophene-containing analogues due to the planarity of the fused thiophene rings, the noncovalent functionalization of carbon nanotubes with dithieno[3,2-*b*:2′,3′-*d*]pyrrole (DTP)-containing conjugated polymers has not been reported.

Received: July 14, 2011
Revised: October 17, 2011
Published: November 02, 2011

Conjugated polymers containing dithieno[3,2-*b*:2′,3′-*d*]pyrrole (DTP) units exhibit lower band gaps when compared to the alkylthiophene-containing analogues due to better π-conjugation across the fused thiophene rings.[39−46] In addition, the conjugated polymers having DTP units in their backbone exhibit interesting optoelectronic properties, making them potentially useful in a variety of device applications including field effect transistors,[39,47] photovoltaic cells,[41,44] and other optoelectronic devices.[45,46,48] Furthermore, it has been shown that the optoelectronic properties of the DTP containing polymers can be easily tailored by altering the composition of the polymer backbone and side chains.[39,46,49] In an attempt to produce a new type of functional nanostructure, we have focused our attention on supramolecular functionalization of carbon nanotubes with DTP and fluorene-containing conjugated polymers. In order to improve the solubility of the resulting polymers and their supramolecular complexes with SWNTs, the polymer backbone was composed of DTP and fluorene units having long alkyl side chains, and two copolymers were prepared that have an identical aromatic backbone but differ in the solubilizing substituents. Here we report the full details of the monomer and polymer preparation, studies of the supramolecular complex formation properties of these polymers with SWNTs, and complete optoelectronic and photophysical characterization of the resulting materials. The effect of changing side chains of the polymer on the interaction between polymer and nanotubes was also investigated.

Scheme 1. Synthetic Routes to Monomer 4

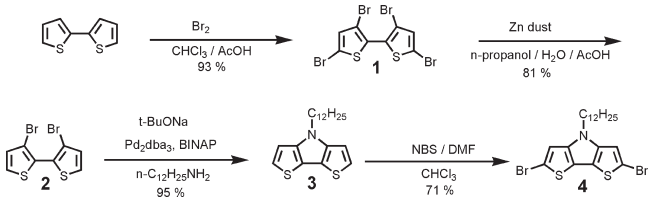

RESULTS AND DISCUSSION

Schemes 1 and 2 show the synthetic route to the target monomers. 3,3′-Dibromo-2,2′-bithiophene (**2**) was synthesized according to literature procedures starting from bithiophene in two steps.[50,51] 3,4,5-Tri(*n*-dodecyloxy)aniline (**7**) was prepared according to a slightly modified literature procedure starting from 1,2,3-trihydroxybenzene.[19,52−54] The *N*-substituted dithieno[3,2-*b*:2′,3′-*d*]pyrrole precursors (compounds **3** and **8**) were prepared from primary amines and 3,3′-dibromo-2,2′-bithiophene using the Buchwald−Hartwig reaction.[41,47,55] In both cases the reactions were carried out in toluene under reflux overnight, with 2,2′-bis(diphenylphosphino)-1,1′-binaphthyl (BINAP) as the ligand and tris(dibenzylideneacetone)dipalladium(0)

Table 1. Molecular Weight and Polydispersity Index Values for the Synthesized Polymers

polymer	M_n (kg/mol)[a]	PDI	M_n (kg/mol)[b]
PF-DTP1	10.8	6.1[c]	11.0
PF-DTP2	18.5	6.2[c]	14.5

[a] Measured by GPC. [b] Estimated by NMR. [c] GPC chromatogram of the polymers showed a broad bimodal distribution.

Scheme 2. Synthetic Routes to Monomer 9

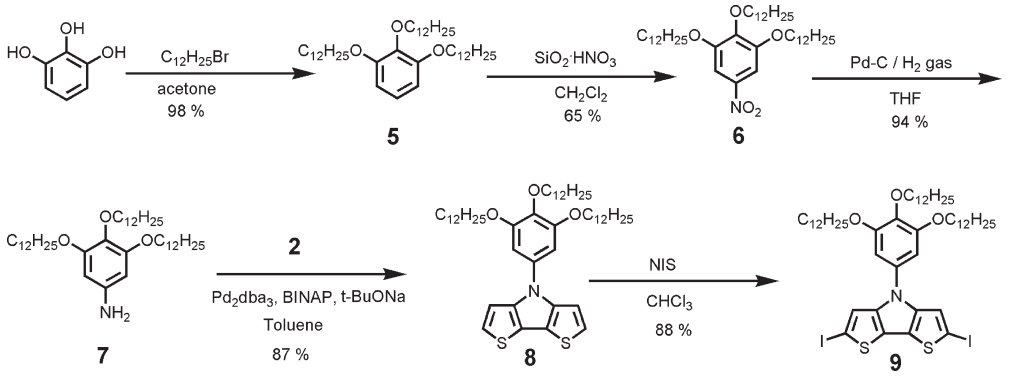

Scheme 3. Synthetic Route to the Polymers

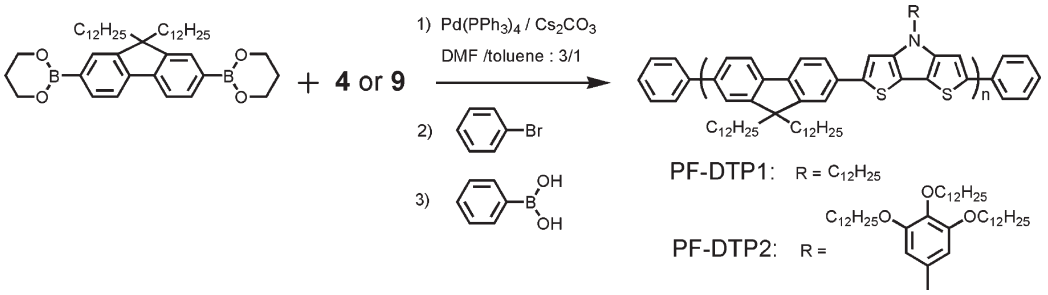

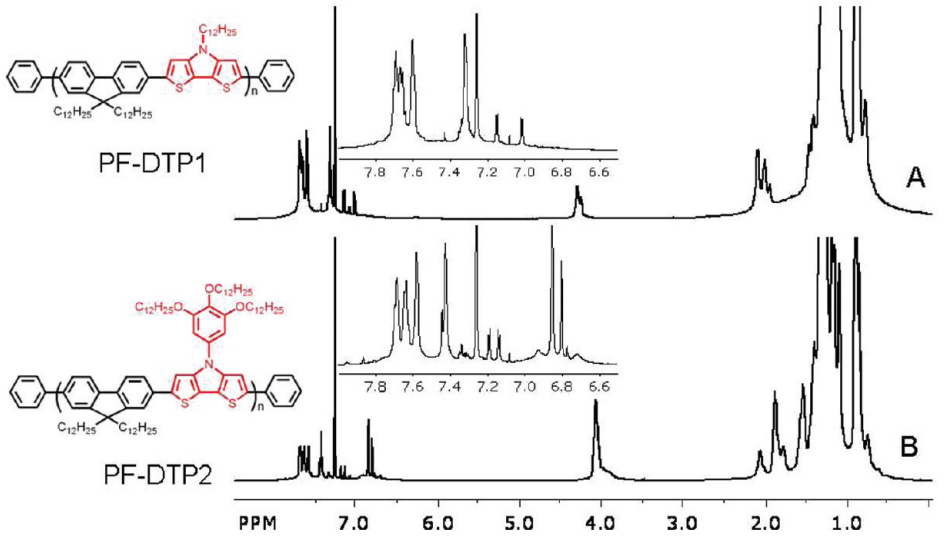

Figure 1. ^{1}H NMR spectra of the polymers in $CDCl_3$. Insets show magnified view of the aromatic (6.5−7.9 ppm) regions.

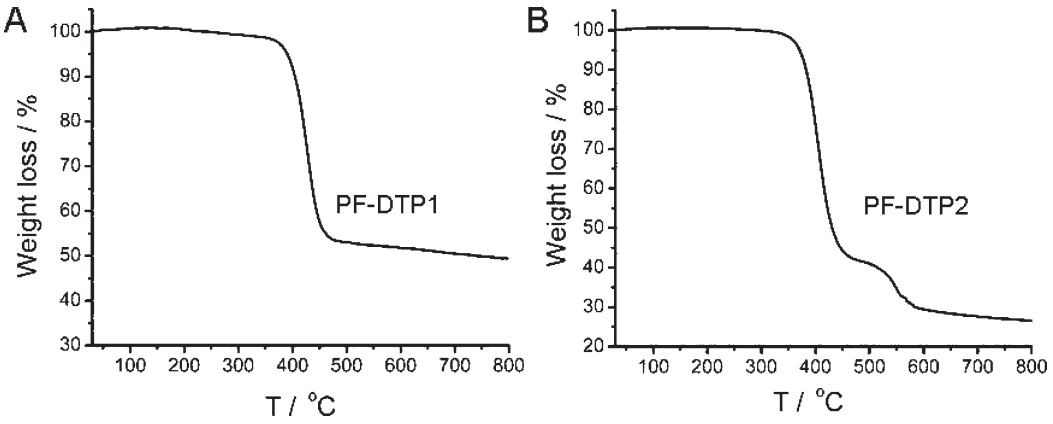

Figure 2. Thermograms of PF-DTP1 (A) and PF-DTP2 (B) measured under an Ar atmosphere.

($Pd_2(dba)_3$) as the Pd source. The reaction products were isolated by simple column chromatography with high yields. By using a slight excess of dodecylamine, we were able to obtain *N*-dodecyldithieno[3,2-*b*:2′,3′-*d*]pyrrole (DTP) (compound **3**) in over 95% yield. When *N*-dodecyldithieno[3,2-*b*:2′,3′-*d*]-pyrrole was treated with *N*-bromosuccinimide (NBS) in $CHCl_3$/DMF at 0 °C, the target compound 2,6-dibromo-*N*-dodecyldithieno[3,2-*b*:2′,3′-*d*] pyrrole (compound **4**) was successfully synthesized in 71% yield.[56] However, when a similar reaction procedure was followed for compound **8**, the bromination occurred not only at the 2- and 6-positions of the DTP ring but also on the phenyl ring due to the presence of the three activating alkoxy groups. We therefore investigated iodination as an alternative, more regioselective route to the desired monomer. The diiodo-substituted *N*-3,4,5(*n*-dodecyloxy)phenyldithieno-[3,2-*b*:2′,3′-*d*]pyrrole was successfully synthesized using *N*-iodo-succinimide (NIS) in $CHCl_3$ at 0 °C.[52]

The polymers PF-DTP1 and PF-DTP2 were prepared using a Suzuki polycondensation from 9,9-didodecylfluorene-2,7-bis-(trimethyleneboronate) and the corresponding *N*-substituted dithieno[3,2-*b*:2′,3′-*d*]pyrrole monomers (compounds **4** and **9**, respectively), as depicted in Scheme 3.[27,29] Preparation of these polymers was performed in a mixture of DMF and toluene (3:1 v/v) as the solvent and tetrakis(triphenylphosphine) palladium ($Pd(PPh_3)_4$) as the polymerization catalyst. In both cases polymers were obtained as orange solids in yields of over 80%. The crude polymers were purified by precipitation twice in methanol. Both polymers exhibited excellent solubility in common organic solvents such as THF, chloroform, and dichlorobenzene at room temperature, which can be attributed to the bulky side chains. Molecular weights of the polymers were determined by gel permeation chromatography (GPC) with polystyrene standards and a mixture of THF and 1% of acetonitrile as the mobile phase. The molecular weight (M_n) and polydispersity index (PDI) values of the polymers are listed in Table 1.

The chemical structures of polymers (PF-DTP1 and PF-DTP2) were confirmed by ^{1}H NMR spectroscopy (Figure 1). The single peak at 7.32 ppm (Figure 1A) corresponds to the aromatic protons from DTP, and the peaks at 7.60−7.66 ppm correspond to the aromatic protons of fluorene. On the basis of the relative areas of these peaks, the molar ratio of fluorene and DTP was determined to be 1:1 in both polymers, which is consistent with the alternating copolymer structure expected from the Suzuki polycondensation of the monomers. Phenyl groups were also successfully introduced at both ends of the polymer as end-caps, and the two sets of doublets at 7.01, 7.15

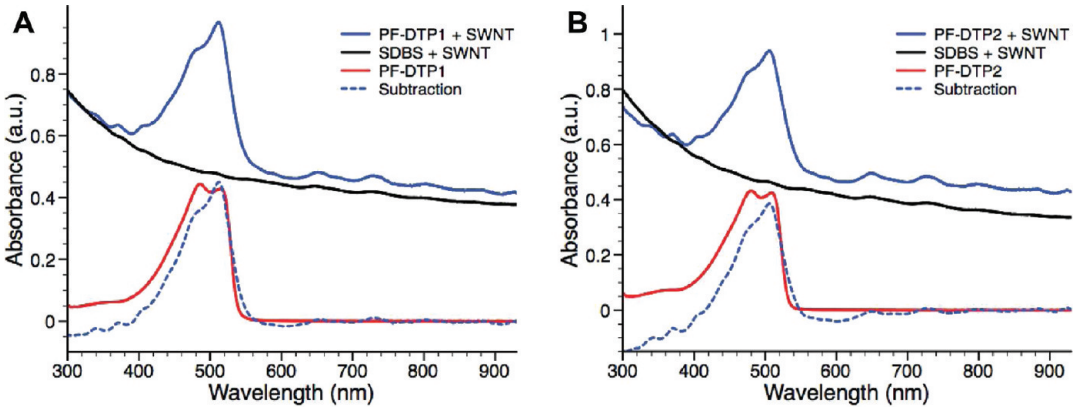

Figure 3. UV−vis absorption data from polymer, SDBS−SWNT, and polymer−SWNT complexes for PF-DTP1 (A) and PF-DTP2 (B).

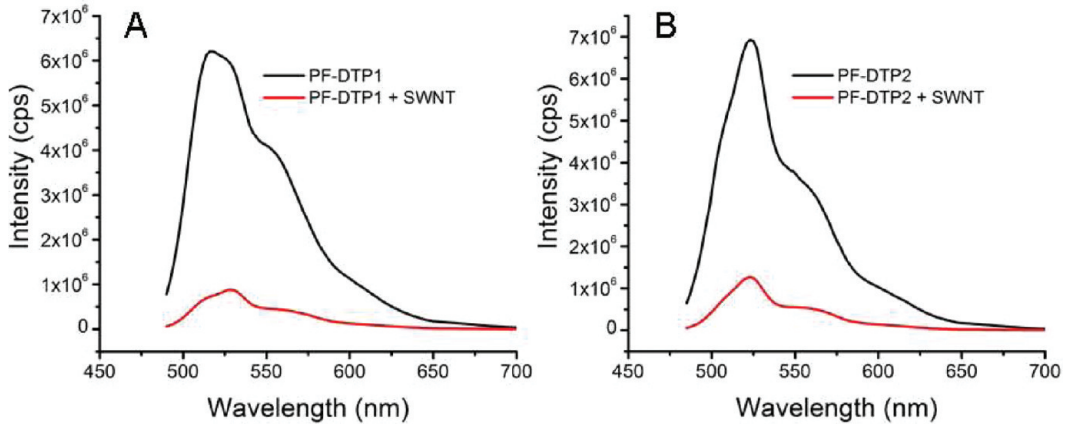

Figure 4. Emission spectra of free polymer and polymer−SWNT complexes using PF-DTP1 (A) and PF-DTP2 (B) polymers, with the excitation wavelength set to the absorption maximum of each sample (485 nm for PF-DTP1 and PF-DTP1 + SWNT; 480 nm for PF-DTP2 and PF-DTP2 + SWNT).

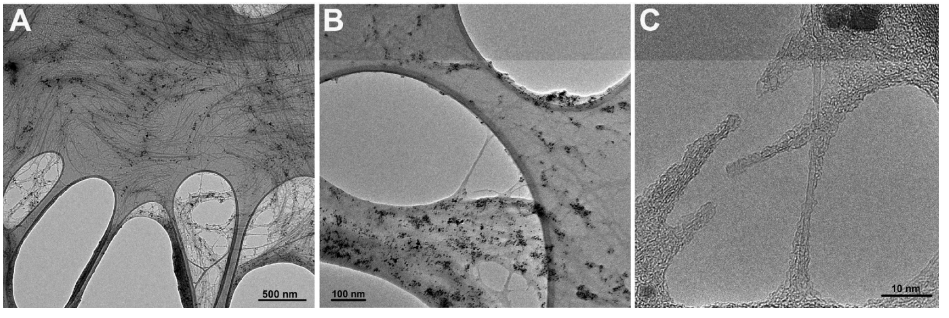

Figure 5. TEM images of PF-DTP1 + SWNT at different magnifications. The high-magnification image clearly shows the presence of individual polymer-wrapped SWNTs. Scale bars are 500 nm (A), 100 nm (B), and 10 nm (C).

ppm for PF-DTP1 and 7.15, 7.20 ppm for PF-DTP2 (Figure 1) were assigned as the end-group phenyl protons.[57] This end-group assignment was also confirmed by the 2-dimensional proton−proton correlation spectrum (^{1}H−^{1}H COSY), heteronuclear single quantum correlation spectrum (^{1}H−^{13}C HSQC), and heteronuclear multiple bond correlation spectrum (^{1}H−^{13}C HMBC) of the PF-DTP1 (see the Supporting Information, Figures S4−S6). On the basis of the integral ratio of the fluorene proton (or DTP proton) signals in the polymer repeat unit to the end-group proton signal, the average degree of polymerization (DP) and M_n were be estimated. The DP and M_n values were calculated to be 13 and 11.0 kg/mol for PF-DTP1 and 11 and 14.5 kg/mol for PF-DTP2, respectively. It should be noted that, although the two polymers have identical backbone structures, the different side chains impart significant differences to their solubility. Not surprisingly, the larger and branched side chain of PF-DTP2 results in a more easily soluble material. Although both polymers were fully soluble in THF, chloroform, and dichloromethane, dissolution of PF-DTP2 occurred much faster relative to PF-DTP1.

The thermal stability of PF-DTP1 and PF-DTP2 was characterized by thermogravimetric analysis (TGA), carried out under an Ar atmosphere (Figure 2). These data indicate that it is not possible to completely decompose the two polymers by heating to 800 °C under Ar. The major mass loss occurs at 375 °C for PF-DTP1, amounting to 48%, and 365 °C for PF-DTP2, amounting to 59%. These mass losses correspond well with the loss of side chains within these polymers. Interestingly, PF-DTP2 exhibits a second decomposition, amounting to ~8% at 491 °C, which corresponds to the loss of the benzene ring from each repeat unit.

The supramolecular interaction of PF-DTP1 and PF-DTP2 with SWNTs was studied using our previously reported methods.[29] In a typical experiment, a SWNT sample (5 mg) was added to a solution of polymer in THF (15 mg/20 mL), and the mixture was ultrasonicated in a bath sonicator for 1 h. The resulting solution was centrifuged for 45 min at 8300 *g* and allowed to stand overnight. The supernatant was carefully transferred by pipet to another vial, producing dark colored and stable polymer−nanotube complex solutions. The isolated supernatant was further diluted with 50 mL of THF, sonicated for 5 min, filtered through a 200 nm pore diameter Teflon membrane, and repeatedly washed with THF until the filtrate was colorless, ensuring removal of all excess free polymer. 20 mL of THF was added to the recovered SWNT residue, and the vial was further sonicated for 5 min. The resulting dark suspension was centrifuged at 8300 *g* for 30 min and allowed to stand overnight undisturbed. It was found that the resulting polymer−SWNT complexes exhibited very good solubility, and the solutions remained stable for periods of at least 3 months with no observable precipitation.

The UV−vis absorption properties of polymers and their corresponding SWNT complexes were measured at room temperature in THF (Figure 3). Because of the high solubility of the polymer−SWNT complexes, all solutions prepared in THF were diluted more than 20-fold in order to make them suitable for absorption and photoluminescence (PL) studies. For reference, the absorption spectra of just the nanotubes, measured from aqueous suspensions with sodium dodecylbenzenesulfonate (SDBS) surfactant, are also shown in Figure 3. PF-DTP1 and PF-DTP2 exhibited an absorption maximum (λ_{max}) of 485 nm (with a low-energy shoulder at 516 nm) and 480 nm (with a low-energy shoulder at 509 nm) in THF, respectively. The overall absorption profiles of the PF-DTP1 and PF-DTP2 were very similar.[48,49]

From comparison of the polymer−SWNT absorption spectrum and that of the free polymer, it is clear that the absorption characteristics of both polymer and SWNTs are evident in the polymer−SWNT absorption spectra. To emphasize the absorption properties of the nanotube-adsorbed polymer, the nanotube component of the polymer−SWNT complex spectra was subtracted to give the subtraction curves shown in Figure 3 for each of the two polymers (curve labeled "Subtraction"). From these subtraction spectra, it appears that the shoulder peaks at lower energy became much more dominant in polymer−SWNT complexes, relative to the free polymer, most likely because of increased electron delocalization.[48] These results indicate that the polymer backbone becomes more planar on the nanotube surface, leading to an enhanced effective conjugation length within the polymer.[27,29]

The fluorescence spectra of the free polymers and polymer−SWNT complexes were also measured in THF. Both PF-DTP1 and PF-DTP2 exhibited strong emission in solution

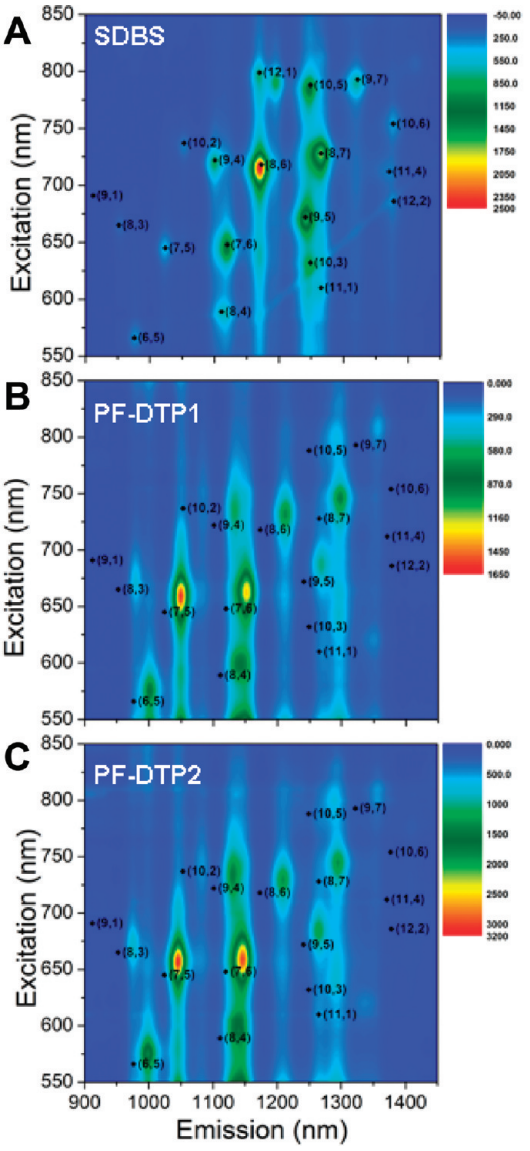

Figure 6. PL contour maps of HiPco SWNTs dispersed with SDBS in D_2O (A), with PF-DTP1 in THF (B), and with PF-DTP2 in THF (C).

(Figure 4). From the normalized emission spectra it is clear that highly efficient quenching of fluorescence occurs when the polymers are adsorbed on the nanotube surface. The fluorescence quenching is likely the result of photoinduced energy or electron transfer between the excited-state conjugated polymer and the SWNT, as previously reported for other systems.[18,31,58]

TEM analysis of the polymer−SWNT complexes revealed the presence of numerous structures resembling individual polymer-coated nanotubes. The high solubility of these complexes in THF allowed deposition and observation of large numbers of SWNT on the TEM grid. However, practically all sample preparation methods resulted in nanotubes localizing on the carbon film of the holey carbon coated TEM grids, diminishing the contrast between the nanotube features and the carbon background. Only a few regions were found with nanotubes spanning holes, where the contrast was great enough for high-resolution imaging. Such images from the PF-DTP1 + SWNT sample are given in Figure 5. In particular, Figure 5C shows the presence of individual, exfoliated SWNTs that are wrapped with polymer chains. From

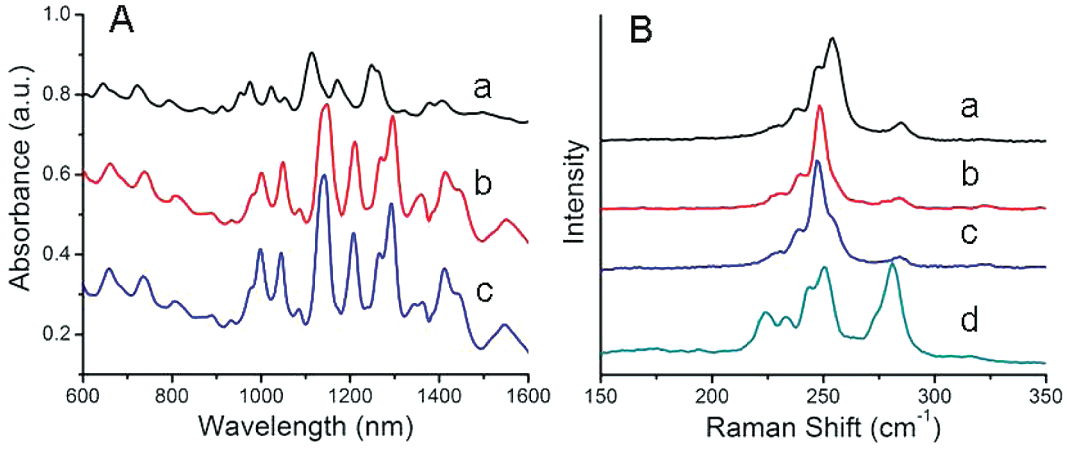

Figure 7. (A) NIR absorption spectra of SDBS/SWNT (a), PF-DTP1 + SWNT (b), and PF-DTP2+SWNT (c). (B) Raman data (with excitation at 785 nm) for SDBS/SWNT (a), PF-DTP1 + SWNT (b), PF-DTP2 + SWNT (c), and pristine SWNT (d), showing only the radial breathing modes of the nanotube samples.

this image, it is clear that nanotubes are separated from bundles by the interaction with the conjugated polymer, consistent with the absorption and emission properties of the polymer−SWNT complexes presented below. For the PF-DTP2 + SWNT sample, the same general features were observed (see Supporting Information, Figure S8), but regions where the sample cleanly spanned a hole could not be found. It should be noted that a large number of iron nanoparticles were also observed within the sample, which are introduced during the synthesis of the raw HiPco SWNTs that were used in this study without any purification.

Photoluminescence excitation maps (PLE) of the samples were measured over a large range of excitation (300−900 nm) and emission (900−1450 nm) wavelengths. As the absorption (E_{22}) and emission (E_{11}) properties strongly depend on the type of the carbon nanotubes, the semiconducting species that are present in solution can be easily identified.[59,60] Figure 6 depicts the photoluminescence excitation (PLE) maps of SWNTs dispersed in THF using the DTP containing polymers (PF-DTP1 and PF-DTP2, respectively), which can be compared to the PLE maps of an aqueous dispersion using SDBS. High intensities are displayed in red and low intensities are displayed in blue. The chiral indices (n, m) for the identified species are labeled on the maps, where the assignment was based on the previously reported results from Weisman and co-workers.[59,60] Figure 6A shows the PLE map of the pristine SWNT sample dispersed in D_2O using SDBS, where 17 different semiconducting nanotubes were detected.[20,60] When the same material was mixed with polymers PF-DTP1 and PF-DTP2 in THF, entirely different results were obtained. Figures 6B and 6C depict the PLE maps of the SWNT complexes with PF-DTP1 and PF-DTP2, respectively. The observed strong nanotube emission indicates that individual SWNTs are solubilized and isolated by the polymer and that removal of free polymer by filtration does not result in any rebundling. It was found that both excitation and emission wavelengths of the polymer−SWNT complexes were red-shifted relative to the aqueous solution by 10−30 nm (Table S1), which is consistent with other previously reported comparable systems.[14,20,30,37] It is obvious from the PLE map that both polymers enable solubilization and isolation of eight major species including (7, 5), (7, 6), (8, 6), (8, 7), (9, 4), (9, 5), (6, 5), and (8, 4) in THF, and the relative emission intensity of each solubilized species is slightly different when a different polymer was used (see Table S2, where the most intense signal of each dispersion was set to a value of 1, and the normalized PLE signal intensities were calculated accordingly). The dominant species within these solutions were found to be (7, 5) and (7, 6) for both polymer−SWNT complexes. Interestingly, signals for both of these nanotube types were not very intense in the PLE maps of the SDBS−SWNT sample in aqueous solution. These results indicate that both polymers may preferentially select nanotubes with a certain diameter range (0.76−1.03 nm).

UV−vis-NIR absorption studies were performed on polymer−SWNT complex solutions in THF as well as the aqueous solution of SWNTs dispersed using SDBS. The UV−vis−NIR absorption spectra are depicted in Figure 7A. The absorption spectrum exhibited features that correspond to the first (E_{11}) and second (E_{22}) interband transitions for semiconducting tubes, which are found from 900 to 1600 nm and 600 to 900 nm, respectively.[61,49] The absorption peaks of the polymer−SWNT complexes become better resolved (Figure 7A, curves b and c) and showed relatively stronger semiconducting transitions when compared to the absorption spectrum of SWNTs dispersed in D_2O using SDBS (Figure 7A,a). All of the transitions of polymer−SWNT complexes were found to be red-shifted more than 20 nm relative to the aqueous solution, which is consistent to what was observed in the photoluminescence maps and has been reported previously with comparable polymers.[20,30,37] The overall absorption profiles of the polymer−SWNT complexes for both polymers (PF-DTP1 and PF-DTP2) are nearly identical.

Raman spectroscopy was used to further characterize the polymer−SWNT samples. Sample preparation involved drop-casting dilute polymer−SWNT solutions in THF onto a glass microscope slide and air-drying prior to measurement. Raman measurements were performed in air, using an excitation wavelength of 785 nm (Supporting Information Figure S7). It has been reported that the radial breathing mode (RBM) profiles at this excitation wavelength can be used as a valuable tool for evaluating the extent of aggregation occurring in a sample.[62,63] RBM profiles of the as-received HiPco sample, SDBS−SWNT, as well as the soluble polymer−SWNT complexes are shown in Figure 7B. The pristine Hipco SWNTs have five major RBM bands at Raman frequencies of ∼281, 250, 243, 233, and 229 cm^{-1} (Figure 7B,d), which is consistent with what has been observed previously with Hipco nanotubes.[62−65] Small shifts and

significant changes in intensity of various bands can be observed when comparing the RBM signals of the solubilized samples to the as received SWNTs. All of the peaks of the polymer−SWNT complexes and SWNT−SDBS show a characteristic red shift of 3−6 cm^{-1} (284, 254, 247, 239, 230 cm^{-1}) relative to the equivalent peaks in the spectrum of the starting material. The signal at 284 cm^{-1} is much more dominant in spectra of pristine bundled SWNTs, and this feature nearly disappeared in the polymer functionalized samples as well as the SDBS dispersed sample. This result indicates that the nanotubes are individually dispersed by polymers in solution, and there is no evidence of aggregation when they are drop-cast onto the glass substrate. Interestingly, both polymer−SWNT complexes exhibit a strong signal at 247 cm^{-1} (corresponding to diameters of ∼0.96 nm), indicating that both polymers selectively bring a specific nanotube species into resonance when excited at 785 nm.

CONCLUSION

We have successfully synthesized a new class of highly soluble alternating copolymers of fluorene and dithieno[3,2-*b*:2′,3′-*d*]pyrrole (DTP). Thermogravimetric analysis indicated that both polymers exhibit excellent thermal stability under Ar. The resulting polymers were subsequently utilized for the preparation of supramolecular polymer−SWNT composite materials, and excellent nanotube solubility and solution stability was achieved. UV−vis absorption measurements revealed a bathochromic shift in the polymer absorption spectrum as a result of complex formation with nanotubes. Flourescence measurements showed that polymer emission is highly quenched in the corresponding SWNT complexes. Both TEM and photoluminescence experiments showed that efficient and selective dispersal of SWNT is possible by using the DTP and fluorene containing copolymers. UV−vis−NIR, photoluminescence, and Raman measurements indicated that the SWNTs were successfully debundled and isolated by polymer in solution, and removal of the free polymer by filtration did not cause further bundling.

ASSOCIATED CONTENT

Supporting Information. Full experimental details, ^{1}H NMR spectra of the monomers **4**, **8**, and **9**, 2D COSY, HSQC, HMBC spectra of PF-DTP1, and Raman spectra; tables of the relative content of the identified nanotube species from the PLE maps. This material is available free of charge via the Internet at http://pubs.acs.org.

AUTHOR INFORMATION

Corresponding Author

*Tel: (905) 525-9140 x23514. Fax: (905) 521-2773. E-mail: adronov@mcmaster.ca.

ACKNOWLEDGMENT

Financial support for this work was provided by the Natural Science and Engineering Research Council of Canada (NSERC), the NSERC Photovoltaic Innovation Network, the Canada Foundation for Innovation (CFI), and the Ontario Innovation Trust (OIT). The authors thank Ms. Julia Huang and Dr. Andreas Korinek for their help with electron microscopy, which was performed in the Canadian Centre for Electron Microscopy (CCEM). P.I. gratefully acknowledges the Ontario Ministry of Training for an Ontario Graduate Scholarship (OGS).

REFERENCES

(1) Iijima, S. *Nature* **1991**, *354*, 56–58.
(2) Ajayan, P. M.; Tour, J. M. *Nature* **2007**, *447*, 1066–1068.
(3) Zhang, D. H.; Ryu, K.; Liu, X. L.; Polikarpov, E.; Ly, J.; Tompson, M. E.; Zhou, C. W. *Nano Lett.* **2006**, *6*, 1880–1886.
(4) Wu, Z. C.; Chen, Z. H.; Du, X.; Logan, J. M.; Sippel, J.; Nikolou, M.; Kamaras, K.; Reynolds, J. R.; Tanner, D. B.; Hebard, A. F.; Rinzler, A. G. *Science* **2004**, *305*, 1273–1276.
(5) Baughman, R. H.; Zakhidov, A. A.; de Heer, W. A. *Science* **2002**, *297*, 787–792.
(6) Wang, F.; Gu, H. W.; Swager, T. M. *J. Am. Chem. Soc.* **2008**, *130*, 5392–5393.
(7) Rahman, M. M.; Umar, A.; Sawada, K. *Sens. Actuators, B* **2009**, *137*, 327–333.
(8) Pang, X.; Imin, P.; Zhitomirsky, I.; Adronov, A. *Macromolecules* **2010**, *43*, 10376–10386.
(9) Artukovic, E.; Kaempgen, M.; Hecht, D. S.; Roth, S.; GrUner, G. *Nano Lett.* **2005**, *5*, 757–760.
(10) Jensen, K.; Weldon, J.; Garcia, H.; Zettl, A. *Nano Lett.* **2007**, *7*, 3508–3511.
(11) Rutherglen, C.; Burke, P. *Nano Lett.* **2007**, *7*, 3296–3299.
(12) Rowell, M. W.; Topinka, M. A.; McGehee, M. D.; Prall, H. J.; Dennler, G.; Sariciftci, N. S.; Hu, L. B.; Gruner, G. *Appl. Phys. Lett.* **2006**, *88*, 233506(233501–233503).
(13) Kymakis, E.; Amaratunga, G. A. J. *Rev. Adv. Mater. Sci.* **2005**, *10*, 300–305.
(14) Schuettfort, T.; Nish, A.; Nicholas, R. J. *Nano Lett.* **2009**, *9*, 3871–3876.
(15) Saito, Y.; Nishiyama, T.; Kato, T.; Kondo, S.; Tanaka, T.; Yotani, J.; Uemura, S. *Mol. Cryst. Liq. Cryst.* **2002**, *387*, 303–310.
(16) Bahun, G. J.; Cheng, F. Y.; Homenick, C. M.; Lawson, G.; Zhu, J.; Adronov, A. *The Polymer Chemistry of Carbon Nanotubes in Chemistry of Carbon Nanotubes*; American Scientific Publisher: Stevenson Ranch, CA, 2008; Vol. 2.
(17) Hirsch, A. *Angew. Chem., Int. Ed.* **2002**, *41*, 1853–1859.
(18) Chen, J.; Liu, H. Y.; Weimer, W. A.; Halls, M. D.; Waldeck, D. H.; Walker, G. C. *J. Am. Chem. Soc.* **2002**, *124*, 9034–9035.
(19) Cheng, F. Y.; Adronov, A. *Chem.—Eur. J.* **2006**, *12*, 5053–5059.
(20) Hwang, J. Y.; Nish, A.; Doig, J.; Douven, S.; Chen, C. W.; Chen, L. C.; Nicholas, R. J. *J. Am. Chem. Soc.* **2008**, *130*, 3543–3553.
(21) Umeyama, T.; Kadota, N.; Tezuka, N.; Matano, Y.; Imahori, H. *Chem. Phys. Lett.* **2007**, *444*, 263–267.
(22) Rice, N. A.; Soper, K.; Zhou, N. Z.; Merschrod, E.; Zhao, Y. M. *Chem. Commun.* **2006**, 4937–4939.
(23) Massuyeau, F.; Aarab, H.; Mihut, L.; Lefrant, S.; Faulques, E.; Wery, J.; Mulazzi, E.; Perego, R. *J. Phys. Chem. C* **2007**, *111*, 15111–15118.
(24) Kang, Y. K.; Lee, O. S.; Deria, P.; Kim, S. H.; Park, T. H.; Bonnell, D. A.; Saven, J. G.; Therien, M. J. *Nano Lett.* **2009**, *9*, 1414–1418.
(25) Goh, R. G. S.; Bell, J. M.; Motta, N.; Waclawik, E. R. *J. Nanosci. Nanotechnol.* **2006**, *6*, 3929–3933.
(26) Casagrande, T.; Imin, P.; Cheng, F. Y.; Botton, G. A.; Zhitomirsky, I.; Adronov, A. *Chem. Mater.* **2010**, *22*, 2741–2749.
(27) Imin, P.; Cheng, F. Y.; Adronov, A. *Polym. Chem.* **2011**, 411–416.
(28) Wu, K. M.; Imin, P.; Adronov, A.; Zhitomirsky, I. *Mater. Chem. Phys.* **2010**, *125*, 210–218.
(29) Cheng, F. Y.; Imin, P.; Maunders, C.; Botton, G.; Adronov, A. *Macromolecules* **2008**, *41*, 2304–2308.
(30) Nish, A.; Hwang, J. Y.; Doig, J.; Nicholas, R. J. *Nature Nanotechnol.* **2007**, *2*, 640–646.
(31) Nish, A.; Hwang, J. Y.; Doig, J.; Nicholas, R. J. *Nanotechnology* **2008**, *19*, 095603 (095601–095606).
(32) Ikeda, A.; Nobusawa, K.; Hamano, T.; Kikuchi, J. *Org. Lett.* **2006**, *8*, 5489–5492.

(33) Tsukamoto, J.; Mata, J. *Jpn. J. Appl. Phys., Part 2* **2004**, *43*, 214–216.
(34) Goh, R. G. S.; Motta, N.; Bell, J. M.; Waclawik, E. R. *Appl. Phys. Lett.* **2006**, *88*, 053101(053101–053103).
(35) Singh, I.; Bhatnagar, P. K.; Mathur, P. C.; Kaur, I.; Bharadwaj, L. M.; Pandey, R. *Carbon* **2008**, *46*, 1141–1144.
(36) Imin, P.; Cheng, F. Y.; Adronov, A. *Polym. Chem.* **2011**, 1404–1408.
(37) Chen, F. M.; Wang, B.; Chen, Y.; Li, L. J. *Nano Lett.* **2007**, *7*, 3013–3017.
(38) Lemasson, F. A.; Strunk, T.; Gerstel, P.; Hennrich, F.; Lebedkin, S.; Barner-Kowollik, C.; Wenzel, W.; Kappes, M. M.; Mayor, M. *J. Am. Chem. Soc.* **2011**, *133*, 652–655.
(39) Liu, J. Y.; Zhang, R.; Sauve, G.; Kowalewski, T.; McCullough, R. D. *J. Am. Chem. Soc.* **2008**, *130*, 13167–13176.
(40) Steckler, T. T.; Zhang, X.; Hwang, J.; Honeyager, R.; Ohira, S.; Zhang, X. H.; Grant, A.; Ellinger, S.; Odom, S. A.; Sweat, D.; Tanner, D. B.; Rinzler, A. G.; Barlow, S.; Bredas, J. L.; Kippelen, B.; Marder, S. R.; Reynolds, J. R. *J. Am. Chem. Soc.* **2009**, *131*, 2824–2826.
(41) Zhou, E. J.; Nakamura, M.; Nishizawa, T.; Zhang, Y.; Wei, Q. S.; Tajima, K.; Yang, C. H.; Hashimoto, K. *Macromolecules* **2008**, *41*, 8302–8305.
(42) Ogawa, K.; Rasmussen, S. C. *Macromolecules* **2006**, *39*, 1771–1778.
(43) Koeckelberghs, G.; De Cremer, L.; Persoons, A.; Verbiest, T. *Macromolecules* **2007**, *40*, 4173–4181.
(44) Yue, W.; Zhao, Y.; Shao, S. Y.; Tian, H. K.; Xie, Z. Y.; Geng, Y. H.; Wang, F. S. *J. Mater. Chem.* **2009**, *19*, 2199–2206.
(45) Zhang, X.; Steckler, T. T.; Dasari, R. R.; Ohira, S.; Potscavage, W. J.; Tiwari, S. P.; Coppee, S.; Ellinger, S.; Barlow, S.; Bredas, J.-L.; Kippelen, B.; Reynolds, J. R.; Marder, S. R. *J. Mater. Chem.* **2010**, *20*, 123–134.
(46) Zhang, X.; Shim, J. W.; Tiwari, S. P.; Zhang, Q.; Norton, J. E.; Wu, P.-T.; Barlow, S.; Jenekhe, S. A.; Kippelen, B.; edas, J.-L. B.; Marder, S. R. *J. Mater. Chem.* **2011**, *21*, 4971–4982.
(47) Zhang, W.; Li, J.; Zou, L.; Zhang, B.; Qin, J. G.; Lu, Z. S.; Poon, Y. F.; Chan-Park, M. B.; Li, C. M. *Macromolecules* **2008**, *41*, 8953–8955.
(48) Evenson, S. J.; Mumm, M. J.; Pokhodnya, K. I.; Rasmussen, S. C. *Macromolecules* **2011**, *44*, 835–841.
(49) Zhang, W.; Li, J.; Zhang, B.; Qin, J. G. *Macromol. Rapid Commun.* **2008**, *29*, 1603–1608.
(50) Khor, E.; Siu, C. N.; Hwee, C. L.; Chai, S. *Heterocycles* **1991**, *32*, 1805–1812.
(51) Liao, L.; Cirpan, A.; Chu, Q. H.; Karasz, F. E.; Pang, Y. *J. Polym. Sci., Part A: Polym. Chem.* **2007**, *45*, 2048–2058.
(52) Vanormelingen, W.; Van den Bergh, K.; Verbiest, T.; Koeckelberghs, G. *Macromolecules* **2008**, *41*, 5582–5589.
(53) Percec, V.; Aqad, E.; Peterca, M.; Rudick, J. G.; Lemon, L.; Ronda, J. C.; De, B. B.; Heiney, P. A.; Meijer, E. W. *J. Am. Chem. Soc.* **2006**, *128*, 16365–16372.
(54) Yelamaggad, C. V.; Achalkumar, A. S.; Rao, D. S. S.; Prasad, S. K. *J. Org. Chem.* **2007**, *72*, 8308–8318.
(55) Koeckelberghs, G.; De Cremer, L.; Vanormelingen, W.; Dehaen, W.; Verbiest, T.; Persoons, A.; Samyn, C. *Tetrahedron* **2005**, *61*, 687–691.
(56) Uwe, L. L. Dithienopyrrole-containing copolymers. US 2008/0262183 A1, 2008.
(57) Yokoyama, A.; Suzuki, H.; Kubota, Y.; Ohuchi, Kazuei; Higashimura, H.; Yokozawa, T. *J. Am. Chem. Soc.* **2007**, *129*, 7236–7237.
(58) Chen, F.; Zhang, W.; Jia, M.; Wei, L.; Fan, X.-F.; Kuo, J.-L.; Chen, Y.; Chan-Park, M. B.; Xia, A.; Li, L.-J. *J. Phys. Chem. C* **2009**, *113*, 14946–14952.
(59) Bachilo, S. M.; Strano, M. S.; Kittrell, C.; Hauge, R. H.; Smalley, R. E.; Weisman, R. B. *Science* **2002**, *298*, 2361–2366.
(60) Weisman, R. B.; Bachilo, S. M. *Nano Lett.* **2003**, *3*, 1235–1238.
(61) Kim, W. J.; Usrey, M. L.; Strano, M. S. *Chem. Mater.* **2007**, *19*, 1571–1576.
(62) O'Connell, M. J.; Sivaram, S.; Doorn, S. K. *Phys. Rev. B* **2004**, *69*, 235415(235411–235415).
(63) Heller, D. A.; Barone, P. W.; Swanson, J. P.; Mayrhofer, R. M.; Strano, M. S. *J. Phys. Chem. B* **2004**, *108*, 6905–6909.
(64) Backes, C.; Schmidt, C. D.; Hauke, F.; Bottcher, C.; Hirsch, A. *J. Am. Chem. Soc.* **2009**, *131*, 2172–2184.
(65) Yang, Q. H.; Gale, N.; Oton, C. J.; Li, F.; Vaughan, A.; Saito, R.; Nandhakumar, I. S.; Tang, Z. Y.; Cheng, H. M.; Brown, T.; Loh, W. H. *Nanotechnology* **2007**, *18*, 405701–405706.